esa

ECOSPHERE

Integrating multiple genetic detection methods to estimate population density of social and territorial carnivores

SEAN M. MURPHY [1,5,†] BEN C. AUGUSTINE,[2,6] JENNIFER R. ADAMS,[3] LISETTE P. WAITS,[3] AND JOHN J. COX[4]

[1]*Louisiana Department of Wildlife and Fisheries, Large Carnivore Program, Lafayette, Louisiana 70506 USA*
[2]*Department of Fish and Wildlife Conservation, Virginia Polytechnic Institute and State University, Blacksburg, Virginia 24061 USA*
[3]*Laboratory for Ecological, Evolutionary and Conservation Genetics, Department of Fish and Wildlife Sciences, University of Idaho, Moscow, Idaho 83844 USA*
[4]*Department of Forestry and Natural Resources, University of Kentucky, Lexington, Kentucky 40546 USA*

Citation: Murphy, S. M., B. C. Augustine, J. R. Adams, L. P. Waits, and J. J. Cox. 2018. Integrating multiple genetic detection methods to estimate population density of social and territorial carnivores. Ecosphere 9(10):e02479. 10.1002/ecs2.2479

Abstract. Spatial capture–recapture models can produce unbiased estimates of population density, but sparse detection data often plague studies of social and territorial carnivores. Integrating multiple types of detection data can improve estimation of the spatial scale parameter (σ), activity center locations, and density. Noninvasive genetic sampling is effective for detecting carnivores, but social structure and territoriality could cause differential detectability among population cohorts for different detection methods. Using three observation models, we evaluated the integration of genetic detection data from noninvasive hair and scat sampling of the social and territorial coyote (*Canis latrans*). Although precision of estimated density was improved, particularly if sharing σ between detection methods was appropriate, posterior probabilities of σ and posterior predictive checks supported different σ for hair and scat observation models. The resulting spatial capture–recapture model described a scenario in which scat-detected individuals lived on and around scat transects, whereas hair-detected individuals had larger σ and mostly lived off of the detector array, leaving hair but not scat samples. A more supported interpretation is that individual heterogeneity in baseline detection rates (λ_0) was inconsistent between detection methods, such that each method disproportionately detected different population cohorts. These findings can be attributed to the sociality and territoriality of canids: Residents may be more likely to strategically mark territories via defecation (scat deposition), and transients may be more likely to exhibit rubbing (hair deposition) to increase mate attraction. Although this suggests that reliance on only one detection method may underestimate population density, integrating multiple sources of genetic detection data may be problematic for social and territorial carnivores. These data are typically sparse, modeling individual heterogeneity in λ_0 and/or σ with sparse data is difficult, and positive bias can be introduced in density estimates if individual heterogeneity in detection parameters that is inconsistent between detection methods is not appropriately modeled. Previous suggestions for assessing parameter consistency of σ between detection methods using Bayesian model selection algorithms could be confounded by individual heterogeneity in λ_0 in noninvasive detection data. We demonstrate the usefulness of augmenting those approaches with calibrated posterior predictive checks and plots of the posterior density of activity centers for key individuals.

Key words: abundance; *Canis;* coyote; data integration; density; hair sampling; individual heterogeneity; noninvasive sampling; scat sampling; social; spatial capture–recapture; territorial.

Received 12 March 2018; revised 2 August 2018; accepted 18 September 2018. Corresponding Editor: James W. Cain III.

[5] Present address: Department of Forestry and Natural Resources, University of Kentucky, 102 T.P. Cooper Building, Lexington, Kentucky 40546 USA.
[6] Present address: Atkinson Center for a Sustainable Future, Department of Natural Resources, Cornell University, 111 Fernow Hall, Ithaca, New York 14853 USA.
† **E-mail:** smmurp2@uky.edu

Introduction

Accurately and precisely estimating wildlife demographic parameters is critical to conservation and management decision-making. Population density is an invaluable parameter because it can inform spatial relationships between populations and ecological conditions, thereby permitting comparisons among populations of the same species that occupy different habitats or landscapes (Royle et al. 2014). By using the spatial patterns of detections, accounting for individual heterogeneity in detection probability that arises due to the juxtaposition of animal home ranges and detector locations, and explicitly modeling space use, spatial capture–recapture analytical methods can produce efficient and unbiased estimates of population density (Efford et al. 2004, Royle et al. 2009). An important property of spatial capture–recapture methods is that detection probability is directly linked to the distance between an animal's activity center (i.e., home range center) and detectors via a spatial scale parameter (σ), which is related to the extent of space use (i.e., home range or territory; Royle et al. 2014). Accuracy and precision of density estimates inherently depend on reliable estimation of σ, which requires sufficient spatial recaptures, or instances of single individuals being detected at multiple locations (Royle et al. 2009, 2014, Efford and Mowat 2014). Detection data produced by a single sampling method are often sparse, however, which can erode accuracy and precision of parameter estimates or possibly prevent density estimation entirely. To overcome this issue and improve the estimation of σ, activity center locations, and population density, recent studies have integrated data from >1 detection method. Examples include combining photos from camera trapping and DNA from scat sampling (Gopalaswamy et al. 2012, Sollmann et al. 2013*c*), photos from camera trapping and telemetry data from radio-collars (Sollmann et al. 2013*a*, *b*, Linden et al. 2017), and telemetry data from radio-collars and DNA from hair sampling (Royle et al. 2013, Tenan et al. 2017).

Nevertheless, caution is warranted when integrating multiple sources of detection data in spatial capture–recapture models. The detection function that these models use to convert detection locations to population density is a product of both animal space use and individuals' behavioral interaction with detectors (Royle et al. 2014). Thus, σ estimates between types of detection data should be tested for consistency to avoid biasing density estimates (Popescu et al. 2014, Tenan et al. 2017). For instance, estimates of σ between hair trapping and radio-collar telemetry data from brown bears (*Ursus arctos*) were found to be inconsistent (Tenan et al. 2017), whereas σ estimates between camera trapping and telemetry data from fishers (*Pekania pennanti*) were congruous (Popescu et al. 2014). Even if σ parameters between detection methods cannot be shared because of inconsistency, integrating multiple types of detection data should still improve estimates of animals' activity centers and the precision of density estimates (Gopalaswamy et al. 2012, Sollmann et al. 2013*a*, *b*, *c*, Tenan et al. 2017). However, because data from multiple detection methods may not be independent if detectors are co-located (i.e., >1 detection method at similar spatial locations), dependence between detection methods, if present, must be accounted for to mitigate parameter estimate bias (Clare et al. 2017).

Social and territorial carnivores, such as canids (*Canis* sp.), occur at multiple trophic levels and can have considerable effects on both herbivores and other carnivores (Berger et al. 2008, Levi and Wilmers 2012, Letnic and Ripple 2017). Wide-ranging movements, crypticism, and general avoidance of humans render many canid species challenging to study and manage, particularly those that are regionally or globally imperiled and necessitate conservation intervention (Boitani et al. 2004). North American gray wolves (*Canis lupus*), Mexican gray wolves (*C. l. baileyi*), and red wolves (*C. rufus*) are federally endangered in parts of the United States, whereas coyotes (*C. latrans*) have expanded range and present a number of management challenges in both wildland and urban environments, including hybridization with wolves (Kays et al. 2009, Bohling and Waits 2011). Reliably estimating population density and abundance of wolves and coyotes is imperative to their conservation and management, but these species are notoriously difficult to detect. Although camera trapping is perhaps the most widely used method for noninvasively detecting wildlife (Foster and Harmsen 2012), the lack of individually unique

natural markings (e.g., pelage spotting or striping) on wolves, coyotes, and other canids typically precludes individual identification from photographs. In contrast, noninvasive genetic sampling that capitalizes on the ecological and behavioral characteristics of canids has become an efficient framework for detecting and individually identifying animals. Both coyotes and wolves tend to be highly territorial and strategically defecate to mark and communicate territory extents to conspecifics (Rothman and Mech 1979, Gese and Ruff 1997, Barja and List 2014); therefore, collecting scat samples along travel routes or at rendezvous sites has proven effective (Stansbury et al. 2014, Morin et al. 2016, Piaggio et al. 2016, López-Bao et al. 2018). Furthermore, rubbing in odorous materials, such as carcasses of dead wildlife, is a natural behavioral response of canids (Ryon et al. 1986, Martin and Farge 1988, Heffernan et al. 2007), and collecting hair from lured ground-based rub pads has been used to detect both wolves and coyotes (Ausband et al. 2011).

Noninvasive genetic sampling does have disadvantages, however, including DNA degradation in scat and hair samples that can reduce the total number of detections and spatial recaptures (Waits and Paetkau 2005, Long et al. 2008, Morin et al. 2016). Cohorts of a population may also have differential defecation rates, particularly at locations commonly used to mark and communicate territories among conspecifics. For example, alpha coyotes and wolves often strategically defecate at a higher rate along travel routes, such as roads and trails, and near territory boundaries than betas, juveniles, and nomadic transients (Rothman and Mech 1979, Barrette and Messier 1980, Wells and Bekoff 1981, Gese and Ruff 1997, Allen et al. 1999). In theory, this should introduce individual heterogeneity in baseline detection probability (λ_0), which could cause underestimation of population density in spatial capture–recapture studies that rely solely on scat sampling. Hair samples tend to have higher DNA amplification success rates than scat samples because hair sampling methods snag multiple hairs that collectively contain more DNA than scat (Waits and Paetkau 2005, Long et al. 2008). Few capture–recapture studies have attempted noninvasive hair sampling of coyotes or wolves, but those that have either collected too few samples or required multiple years of sampling to obtain sufficient sample sizes for parameter estimation, potentially violating model assumptions (e.g., population closure; Ausband et al. 2011, Stansbury et al. 2014, Mumma et al. 2015). Consequently, employing only scat or only hair sampling can cause deficiencies that may preclude reliable estimation of demographic parameters. Potential exists for improving estimates of σ, activity center locations, and population density by integrating detection data from simultaneous scat and hair sampling, but the effectiveness of this combination remains unexplored for canids and other social and territorial carnivores in the spatial capture–recapture framework.

Herein, we build on prior spatial capture–recapture studies that integrated multiple sources of detection data by extending this work to noninvasive genetic sampling of social and territorial carnivores. We explicitly evaluated the appropriateness of combining genetic detection data from hair and scat sampling of a common social and territorial carnivore, the coyote, to improve precision of estimated σ, activity center locations, and population density, using a combination of posterior inference, posterior predictive checks, and posterior density plots of activity center locations. The ecological and behavioral characteristics of coyotes overlap that of multiple other social and territorial canids (Moehlman 1989), rendering the species a useful model for investigating this approach.

Materials and Methods

Study area

Our study area was centered on the U.S. Fish and Wildlife Service's Southwest Louisiana National Wildlife Refuge (NWR) Complex in Louisiana, USA, which encompassed Sabine, Lacassine, and Cameron Prairie NWRs (Fig. 1). All lands interspersed between said Refuges were privately owned, some by resource extraction companies. The dominant private land use was agriculture, primarily rice prairies and domestic cattle operations. The study area was in the West Gulf Coastal Plain physiographic region, bordered to the south by the Gulf of Mexico, and was largely comprised of forested wetlands, coastal prairies, cheniers, and freshwater, brackish, and saltwater marshes (Mac et al.

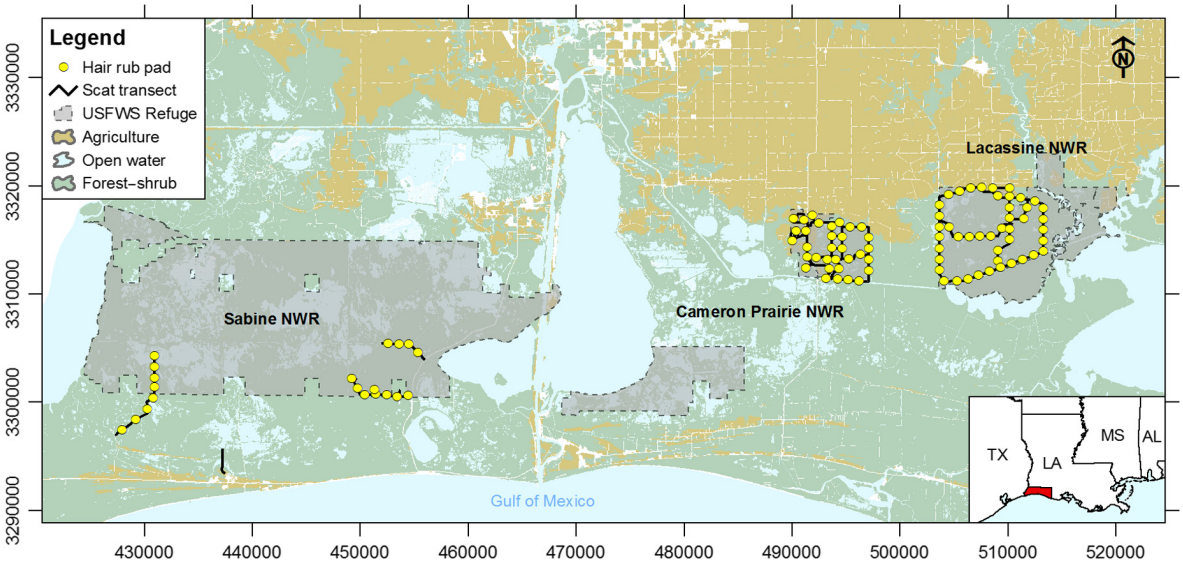

Fig. 1. Locations of 98 hair rub pads (yellow circles) and ~127 km of scat transects (solid black lines) relative to the U.S. Fish and Wildlife Service's (USFWS) Sabine, Cameron Prairie, and Lacassine National Wildlife Refuges (NWR; gray shaded areas). Universal Transverse Mercator coordinates are presented on the axes, and agriculture (brown shaded areas), open water (light blue shaded areas), and forest–shrub cover (green shaded areas) from 2011 National Land Cover Database data (Homer et al. 2015) are presented for context.

1998). The climate was humid subtropical; average monthly precipitation was 12.8 cm; and average monthly temperature was 20.3°C (Mac et al. 1998). Given the low elevation (0–6 m asl) and proximity to the Gulf of Mexico, an extensive network of levees existed that were designed to divert flood waters away from agricultural lands and human population centers. These levees served as efficient travel routes for terrestrial vertebrates (e.g., white-tailed deer [*Odocoileus virginianus*] and bobcat [*Lynx rufus*]).

Noninvasive scat and hair sampling

We established a total of ~127 km of scat sampling transects along gravel and dirt roads, hiking trails, and levees. We first cleared all scat from all transects immediately prior to implementing sampling to equalize the expected baseline detection rates across sampling occasions (Morin et al. 2016). We then surveyed all transects every seven days to collect fecal DNA samples from detected scat, recorded Universal Transverse Mercator coordinates for each scat, and removed all sampled scat from transects to prevent double-sampling. Fecal DNA was obtained by collecting a ~0.5 cm^3 portion of the exterior of each scat using tweezers that were sterilized between sample collections via flame from a lighter to prevent cross-contamination (Stenglein et al. 2010). Each fecal DNA sample was placed in an individually labeled collection tube that contained 1.4 mL of DETS buffer to mitigate DNA degradation (Stenglein et al. 2010, Lonsinger et al. 2015).

Following the methods and recommendations developed by Ausband et al. (2011) for hair sampling both coyotes and wolves, we used ground-based rub pads to noninvasively collect hair samples. We constructed each rub pad by securing three carpet-tack strips to 30.5 × 15.2 cm plywood board that was 1.3 cm thick; all rub pads were constructed ~60 d prior to sampling and were stored away from human activity to minimize the potential influence of human scent on detection. We placed a total of 98 rub pads at ~1.0-km intervals along the scat sampling transects, and we secured each rub pad to the ground using six galvanized nails of size 4 d (3.81 cm long). To elicit a rubbing response, we placed ~5.0 mL of a 1:1 mixture of Government Call (O'Gorman's, Broadus, Montana, USA) and Canine Call (Carman's, New Milford, Pennsylvania, USA) lure on

the exposed surface of each rub pad (Ausband et al. 2011); to avoid a fossorial response that could cause removal or displacement of rub pads by animals, we did not place lure underneath or on the ground surrounding rub pads. We checked and re-lured each rub pad every seven days and collected hair samples using tweezers that were sterilized between sample collections via flame from a lighter; we also sterilized nails on carpet-tack strips between collections using flame. We placed collected hair samples in individually labeled paper coin envelopes, which we stored in silica desiccant to remove moisture and prevent DNA degradation (Stenglein et al. 2010, Ausband et al. 2011).

Scat and hair sampling occurred simultaneously for eight consecutive seven-day sampling occasions from December 2015 to February 2016. Thus, we sampled during the winter coyote breeding season when the probability of detection should have been highest (Long et al. 2008). Because the majority of transects were located in areas that were closed to vehicular access by the public, we did not apply correction factors that may be needed for scat transect sampling that occurs in areas subjected to high scat removal rates (Lonsinger et al. 2016).

Laboratory genetic analyses

Our laboratory analyses of hair and scat samples were nearly identical to those used by Ausband et al. (2011) and Morin et al. (2016), respectively. Briefly, we analyzed samples at the Laboratory for Ecological, Evolutionary and Conservation Genetics at University of Idaho (Moscow, Idaho, USA), which had facilities dedicated to analyzing low-quality, low-quantity DNA samples. We used a mitochondrial DNA fragment analysis to identify species of origin for each scat and hair sample (De Barba et al. 2014). We attempted to generate genotypes for all samples confirmed as originating from coyotes using the following nine microsatellite loci that were multiplexed together: CXX.377, CXX.172, CXX.173, CXX.250, CXX.109, CXX.200, AHT121, AHT103, and CXX.20 (Ostrander et al. 1993, Holmes et al. 1995, Mellersh et al. 1997). The multiplex contained 0.06 μmol/L of CXX.377, 0.07 μmol/L of CXX.172, CXX.173 and CXX.250, 0.13 μmol/L of CXX.109, 0.16 μmol/L of CXX.200, 0.20 μmol/L of AHT121, 0.60 μmol/L of AHT103, 0.71 μmol/L of CXX.20, 1× Qiagen Multiplex PCR Kit Master Mix, 0.5× Q solution, and 1 μL of DNA extract in a 7 μL reaction volume. The thermal profile for the multiplex PCR was 94°C for 10 min followed by 13 cycles of a 63°C annealing temperature, touching down by 0.8°C each cycle, followed by 25 cycles at an annealing temperature of 55°C, and ending with a final extension of 60°C for 30 min. We used a sex identification marker to determine sex (Seddon 2005); this PCR contained 0.10 μmol/L of DBX and 0.07 μmol/L of DBY, 1× Qiagen Multiplex PCR Kit Master Mix, 0.5× Q solution, and 2 μL of DNA extract in a 7 μL reaction volume. The thermal profile for the sex identification PCR was 94°C for 10 min followed by 13 cycles of a 62°C, touching down by 0.4°C each cycle, followed by 27 cycles at an annealing temperature of 57°C, and ending with a final extension of 60°C for 30 min.

Up to four and six PCR replicates were performed for the hair and scat samples, respectively, that consistently amplified after initial screening. We used the genotype screening and sample quality assessment methods described by Adams and Waits (2007) and Stenglein et al. (2010). We used GenAlEx v6.501 (Peakall and Smouse 2012) to calculate probability of identity for siblings ($P_{ID(sibs)}$), or the probability that siblings shared the same genotype by chance, for the nine microsatellite loci. Results indicated that five loci were sufficient to differentiate between individuals ($P_{ID(sibs)} = 0.0082$). We conducted a matching analysis in GenAlEx 6.501, and we considered samples as originating from the same individual if they matched at ≥5 loci.

Spatial capture–recapture and integration of detection data

Although the 98 hair rub pads had fixed locations for the duration of sampling, scat samples were detected at non-fixed locations along transects. Therefore, we discretized scat transects at 500-m intervals to create 264 scat detectors that were assigned the mean coordinates of each interval (Royle et al. 2014, Morin et al. 2016); this discretization distance was determined by sequentially reducing the resolution from 1000 m until the density estimate stabilized (estimates using 250- and 500-m intervals were nearly identical). Each scat sample was then assigned to the scat detector location that

represented the transect interval from which the sample was collected. We defined $\boldsymbol{Y}^h$ and $\boldsymbol{Y}^s$ to be the hair (h) and scat (s) encounter histories, respectively, which consisted of the number of unique detections at each detector for each individual across the $K = 8$ sampling occasions. The encounter histories were of size $n \times J^h$ and $n \times J^s$, where n was the number of individuals detected via hair and/or scat sampling, and J^h and J^s were the number of hair and scat detectors, respectively. We defined $\boldsymbol{X}^h$ and $\boldsymbol{X}^s$ to be the matrices containing the Universal Transverse Mercator coordinates of hair and scat detectors, respectively.

We estimated population density using ordinary spatial capture–recapture models (Royle et al. 2014), except we explored three different observation models: scat-only (SO), a combined scat and hair model that shared σ between detection methods (SH1), and a combined scat and hair model with separate σ for each detection method (SH2). We initially fit the SO model with sex-specific detection function parameters and found that point estimates were nearly identical between sexes (Appendix S1: Table S1); therefore, we pooled sexes for all model fitting. We did not consider sharing λ_0 since there was no obvious reason to expect the two detection methods would have the same baseline detection rate. For each observation process, we assumed that detections of individuals at each location occurred following $y_{ij}^m \sim \text{Binomial}(p_{ij}^m, K)$, for $m \in \{h,s\}$ (hair, scat) after reducing any individual by trap by occasion counts >1 to binary detection events. Note that the i index was shared between the method-specific encounter histories, so individuals that were detected by both methods had detections stored in the same row of each encounter history and individuals not detected by one method had a row of all zeros. We also assumed that the detection probability of an individual at a detector depended on the distance between an individual's activity center and the detector location following a hazard half-normal detection function: $p^m(s_i, x_j^m) = 1 - \exp(-h(s_i, x_j^m))$, where $h^m(s_i, x_j^m) = \lambda_0 \exp(-\frac{\|S_i - x_j^m\|^2}{(2\sigma^m)^2})$. We defined the scat-specific detection function parameters to be λ_0^s and σ^s, the hair-specific detection function parameters to be λ_0^h and σ^h, and the combined (shared) spatial scale parameter to be σ^c. For the process model, we used the typical assumption that N activity centers, s_i, $i = 1,\ldots,$ N, were distributed uniformly across a continuous state space, $\boldsymbol{S}$, such that $s_i \sim \text{Uniform}(\boldsymbol{S})$. The extent of $\boldsymbol{S}$ was defined by buffering the array of combined hair and scat detectors (union of $\boldsymbol{X}^h$ and $\boldsymbol{X}^s$) by 6 km, or ~3σ, which resulted in a total estimation area of 3733 km^2.

We implemented a Bayesian model fitting framework in the R statistical software (v3.5.0; R Core Team 2018) using spatial capture–recapture Markov chain Monte Carlo (MCMC) algorithms with data augmentation to estimate population size (N) and density, the latter of which was calculated as N/A, where A is the area of the state space (Royle et al. 2009, 2014). The level of data augmentation varied from $M = 450$ to 650, depending on the magnitude of uncertainty in population size when using each observation model, where M is the maximum possible number of individuals in the population (Royle et al. 2014). We ran three chains of length 30,000 for each model and discarded the first 5000 as burn-in, except for the SH2 model, for which we ran six chains of length 30,000 with the first 5000 discarded as burn-in. We used the posterior mode for point estimates and the 95% highest posterior density for credible intervals. We compared the precision of the three models using the coefficient of variation (CV), defined as the posterior standard deviation divided by the posterior mode. Although Tenan et al. (2017) described a Bayesian model selection algorithm for testing parameter consistency, we only had two parameters to compare, and thus, we assessed the consistency of σ^h and σ^s using the posterior of $\sigma^h > \sigma^s$. We assumed independence between the partially co-located detection methods (98 of the 264 scat transect intervals contained a hair rub pad) in the SH1 and SH2 observation models (contra Clare et al. 2017) because we did not observe any instances of both scat and hair samples from the same individual occurring during the same sampling occasion in the same scat transect interval, which would be expected to occur if positive dependence existed between detection methods (see *Results*).

We assessed the goodness of fit of our models using Bayesian P-values (Robins et al. 2000) from four test statistics. First, we used the following Freeman-Tukey-based test statistics described by Royle et al. (2014) for both the hair

and scat observation models conditional on $\boldsymbol{s}$, the activity centers, and $\boldsymbol{z}$, the vector indicating which individuals are estimated to be in the population on each MCMC iteration. T1 tested the fit of the individual × detector frequencies, summed over all individuals and detectors; T2 tested the fit of individual-level detection frequencies, summed over all individuals for a single metric of individual-level lack of fit; and T3 tested the fit of the detector-level detection frequencies, summed across detectors for a single metric of detector-level lack of fit. Second, because fewer individuals than expected were detected by both methods ($n = 3$) based on the detection function parameter estimates (see *Results*), we used the test statistic T4, the number of individuals detected by both methods conditional on $\boldsymbol{s}$ and $\boldsymbol{z}$, to calculate a Bayesian *P*-value for $\Pr(T4 \leq 3)$. Because Bayesian *P*-values are generally conservative (Robins et al. 2000), we calculated calibrated Bayesian *P*-values by comparing the observed *P*-value to the expected *P*-value distribution when simulating from the fitted model (Hjort et al. 2006). Due to the computational intensity of generating the expected *P*-value distributions, we limited their size to 96 replications for each SO, SH1, and SH2.

Data, R code for MCMC algorithms, and R code for posterior predictive check algorithms are provided in Data S1. To aid in diagnosing lack of fit, we created two-dimensional plots of the summed posterior density of the activity center locations for individuals that were only detected by the hair rub pads. We excluded one individual in the plots because it was recorded on a smaller section of the detector array (Sabine NWR), further away from the section where the other individuals were detected (Cameron Prairie and Lacassine NWRs), which rendered the posterior densities difficult to visualize due to spatial extent. We used a kernel density estimator with a 500-m bandwidth to create posterior density plots via the R package MASS (Venables and Ripley 2002).

Results

Noninvasive scat and hair sampling

We collected 335 fecal samples from scat transects and 204 hair samples from rub pads. Of those, 244 fecal samples (72.2%) and 107 hair samples (52.4%) either failed to yield sufficient mitochondrial DNA for species identification ($n = 320$) or were from a species other than coyote (bobcat [$n = 29$], domestic cat [*Felis silvestris catus*, $n = 1$], and domestic dog [*C. l. familiaris*, $n = 1$]). Among the remaining 94 fecal samples and 97 hair samples, 40 (42.5%) and 81 (83.5%), respectively, contained insufficient nuclear DNA for amplification of all nine microsatellite loci. This resulted in 22 (13M:9F) unique individuals that were detected 54 times via scat transects (median = 1 detection/individual, range = 1–12), and 13 (8M:5F) unique individuals that were detected 16 times (median = 1 detection/individual, range = 1–3) at 14 different rub pads (14.3% of all rub pads); three individuals (1M:2F) were detected by both scat transects and hair rub pads. Thus, we acquired 70 total detections of 32 (20M:12F) unique individuals; however, we discarded one female that was detected only once by a single hair rub pad because the rub pad identifier was not recorded at the time of collection. A post hoc chi-square test indicated the sex ratio of detected individuals was not significantly different from 1:1 ($\chi^2_1 = 2.00$; $P = 0.16$). After reducing individual by trap by occasion counts >1 to binary detections, there were 49 total scat and 15 total hair detection events. The scat samples provided 24 spatial recaptures from 10 individuals (5M:5F) and the hair samples provided three spatial recaptures from two individuals (1M:1F).

Spatial capture–recapture and integration of detection data

Density estimates from the SO, SH1, and SH2 observation models were 5.49 (95% CI = 3.67–9.67), 9.37 (95% CI = 5.68–14.20), and 8.17 (95% CI = 4.79–12.64) individuals/100 km^2, respectively (Table 1). Integrating hair detections with scat detections improved precision of the density estimate when σ was shared (SH1; CV declined from 0.29 to 0.23), but to a lesser extent when a method-specific σ was estimated (SH2; CV declined from 0.29 to 0.25). The posterior probability of $\sigma^h > \sigma^s$ was 0.89, supporting the hypothesis that the hair detection σ was larger than the scat detection σ. The λ_0^s point and interval estimates most similar to those from model SO were from model SH2, suggesting that sharing σ between detection methods in SH1 introduced

Table 1. Spatial capture–recapture model parameter estimates, lower and upper bounds of 95% credible intervals, and coefficients of variation (CV), from three observation models.

Model and parameter	Estimate	Lower	Upper	CV
SO				
λ_0^s	0.019	0.011	0.032	0.30
σ^s	1512	1275	2234	0.17
N	205	137	361	0.29
D	5.49	3.67	9.67	0.29
SH1				
λ_0^s	0.013	0.009	0.024	0.30
λ_0^h	0.011	0.006	0.022	0.42
σ^c	1590	1256	2048	0.13
N	349	211	529	0.23
D	9.37	5.68	14.20	0.23
SH2				
λ_0^s	0.017	0.009	0.030	0.34
λ_0^h	0.003	0.001	0.019	1.99
σ^s	1497	1250	2085	0.14
σ^h	2468	1020	4897	0.45
N	305	178	471	0.25
D	8.17	4.79	12.64	0.25

Notes: Models were scat-only (SO), combined scat and hair with shared spatial scale of the detection function parameter (SH1), and combined scat and hair with method-specific spatial scale of the detection function parameter (SH2). Estimated model parameters were baseline detection rate (λ_0), spatial scale of the detection function (σ), population size (N), and population density (*D*). Estimates of σ and *D* are in meters and individuals per 100 km^2, respectively. Superscripts denote combined (*c*), hair-only (*h*), and scat-only (*s*) detection function parameters.

negative bias into λ_0^s and positive bias into estimated density. The primary mechanism driving down the SH1 estimate of λ_0^s was that the smaller, shared σ^c estimate moved the activity centers of the individuals that were only detected by hair rub pads closer to the scat transects, where they were not detected (Fig. 2). In contrast, model SH2 estimated σ^h to be larger than σ^s, which allowed the activity centers of the hair-only detected individuals to shift further away from the detectors, thereby increasing estimated λ_0^s, but not to the same magnitude as in model SO, perhaps still positively biasing the density estimate. Although σ estimates were similar between models SO and SH1, the shared σ^c estimate in SH1 likely introduced bias into λ_0^h, which was substantially lower in SH2 that had separate σ parameters (0.012 vs. 0.003, respectively), further suggesting that the shared σ^c estimate in SH1 was inconsistent with the hair detection data.

Calibrated Bayesian *P*-values were generally quite different than the observed Bayesian *P*-values (Table 2), primarily because of the non-uniform distribution of expected Bayesian *P*-values (Appendix S1: Figs. S1–S4). Calibrated Bayesian *P*-values did not indicate lack of fit of model SO; however, evidence existed for lack of fit at the individual level for both scat and hair detections and at the detector level for hair detections in model SH1. Model SH2 had similar evidence for lack of fit as model SH1, except at the individual level for hair detections, which did not support lack of fit and suggested that separate σ parameters for each observation process improved fit for the hair detection model. Lack of fit was supported in T4, the statistic quantifying the number of individuals detected by both methods in both SH1 and SH2, indicating that the observing of three or fewer individuals by both methods was unlikely to occur by random chance if SH1 or SH2 was true.

Discussion

Reliable and precise estimation of demographic parameters for terrestrial carnivores is challenging yet critical to their conservation and management. We found that the precision of population density estimated by spatial capture–recapture models for a social and territorial carnivore was slightly improved when two non-invasive genetic detection data types were integrated (SH1). Further, if our DNA amplification success rate for hair samples had been higher, thereby increasing the number of detections, precision of the density estimate likely would have improved more. Using the posterior probabilities of σ^h and σ^s and posterior predictive checks for each observation process, we found support for differing σ parameters between scat and hair observation models (SH2). This was largely influenced by the nine individuals that were detected via hair rub pads but not scat transects. In model SH1, the activity centers of those individuals were located too close to the scat transects for their lack of detection via scat to be likely, whereas the larger σ for the hair detection process in model SH2 allowed their activity centers to be estimated further from the co-located scat transects, where their lack of detection via scat was more likely (Fig. 2). Because these nine

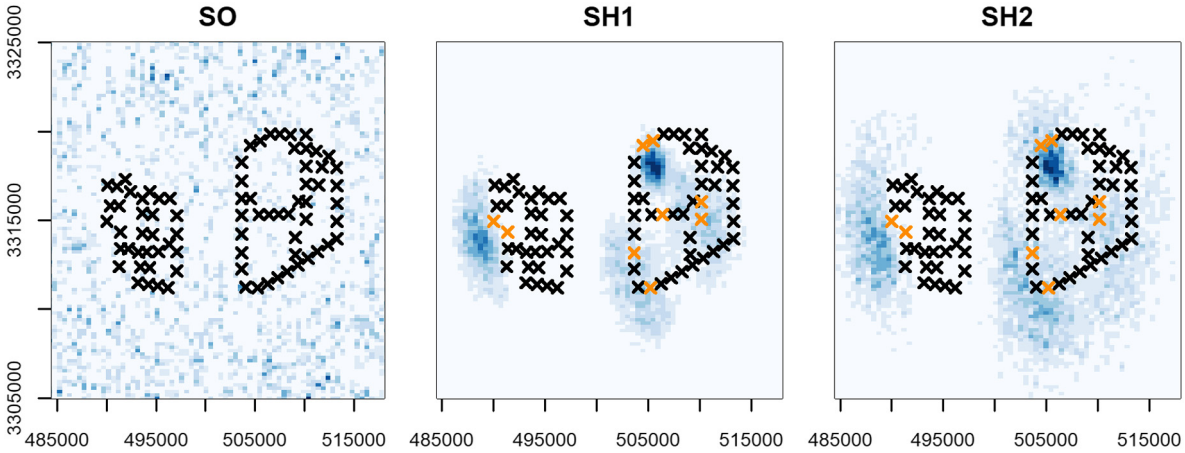

Fig. 2. Activity center posteriors for individuals that were only detected by hair rub pads at Cameron Prairie and Lacassine National Wildlife Refuges, USA (Fig. 1), for the scat-only model (SO), the combined scat and hair detections with shared σ model (SH1), and the combined scat and hair detections without shared σ model (SH2). For model SO, eight random individuals were selected because we could not definitively identify which undetected individuals in model SO were those that were only detected by the hair rub pads. Hair rub pads are denoted by black crosses, the rub pads at which hair samples were collected from the eight individuals are denoted by orange crosses, and Universal Transverse Mercator coordinates are presented on the axes. The area of high posterior mass (dark blue) corresponds to one individual detected three times by the hair rub pads, with the remainder of the posterior mass corresponding to the other seven individuals that each had single detections.

Table 2. Bayesian *P*-values from posterior predictive checks of scat transect and hair rub pad observation models.

Model	*P*-value	T1 Scat	T1 Hair	T2 Scat	T2 Hair	T3 Scat	T3 Hair	T4
SO	Observed	0.47		0.32		0.15		
	Calibrated	0.62		0.48		0.37		
SH1	Observed	0.50	0.52	0.01*	0.17	0.14	0.29	0.03*
	Calibrated	0.53	0.43	<0.01**	0.08	0.03*	0.27	<0.01**
SH2	Observed	0.49	0.54	0.08	0.15	0.17	0.22	0.06
	Calibrated	0.27	0.89	<0.01**	0.65	0.04*	0.83	0.02*

Notes: We evaluated fit of individual × detector frequencies (T1), individual frequencies (T2), detector frequencies (T3), and the number of individuals detected by both sampling methods (T4; *P*-value is the probability ≤3 observed). Models were scat-only (SO), combined scat and hair with shared spatial scale parameter (SH1), and combined scat and hair with method-specific spatial scale parameter (SH2). Asterisks denote statistically significant values ($^{*}P < 0.05$, $^{**}P < 0.01$, $^{***}P < 0.001$).

individuals represent the majority of individuals detected via hair rub pads, model SH2 describes a scenario in which the individuals detected via scat lived on and around transects, but the majority of individuals detected via hair mostly lived off of the detector array and had larger σ, so the latter could come onto the detector array and leave hair samples but not scat samples.

A second explanation for these patterns is individual heterogeneity in λ_0 for one or both detection methods. In the presence of individual heterogeneity in λ_0, spatial capture–recapture models will generally estimate an averaged but positively biased λ_0 (Royle et al. 2014). This pushes the activity centers of the lower λ_{0i} individuals further away from the detector array or into holes in the array where no detectors exist and those individuals are less likely to be detected, thereby accommodating their lower than expected observed detection rate (sensu Murphy et al. 2017). If individual heterogeneity

in λ_0 is only present in one detection method or is method-specific (e.g., the low λ_0^h individuals were not identical to the low λ_0^s individuals), the low λ_{0i} individuals for one detection method cannot be moved further from the trapping array without sacrificing fit of the other observation model. Therefore, when combining multiple types of structured noninvasive detection data, inconsistencies in individual heterogeneity between detection methods can introduce negative bias, rather than the typical positive bias, in the averaged λ_0 estimate. This successively introduces positive bias in density estimates, which is the opposite of what occurs if using a single detection method (Royle et al. 2014).

Tension between the inconsistent individual heterogeneity in λ_0 can be partially alleviated by estimating method-specific σ parameters, which allows the activity centers of individuals with low λ_0 for one detection method to be moved further away from the trapping array where they will be less likely to be detected by the method that has the smaller σ. Thus, robustly testing for parameter consistency between multiple types of structured detection data (e.g., Tenan et al. 2017) may be difficult when individual heterogeneity in λ_0 exists, which is likely prevalent in many types of noninvasive detection data. For terrestrial carnivores that have large spatial requirements, these data will often be too sparse to investigate models with independent or negatively correlated individual heterogeneity in λ_0 between sampling methods, leaving us without a method to reliably combine multiple types of noninvasive detection data.

We found two forms of evidence that favored the hypothesis that individual heterogeneity in λ_0 was inconsistent between detection methods over the hypothesis that the methods had different σ parameters. First, the SO model that excluded the hair detections did not indicate lack of fit (Table 2), whereas both models SH1 and SH2, which had method-specific parameters, demonstrated lack of fit in the scat detection process. Configuring individual activity centers to be consistent with the hair detections essentially made them less consistent with the scat detections, even if σ was not shared. Second, the Bayesian *P*-value for the number of individuals that should have been detected by both methods was significant (<0.01 and 0.02 in models SH1 and SH2, respectively), indicating that we detected fewer individuals than expected by both methods under the respective model assumptions. The only plausible explanation for this result that we are aware of is that one cohort of the population was more susceptible to detection by the hair rub pads and another cohort was more susceptible to detection via scat transects. Thus, inconsistent individual heterogeneity in λ_0 was a more convincing explanation for the patterns in our data than each detection method having a separate σ.

Both explanations for the patterns that we observed, either method-specific σ or differential individual heterogeneity in λ_0, can be attributed to the ecology and behavior of social and territorial canids. Similar to wolves, coyotes form packs of alpha pairs, betas, and offspring that establish and defend territories (i.e., residents; Moehlman 1989). These resident individuals typically have smaller home ranges and movements than do nomadic transients, who are solitary and non-territorial (Kamler and Gipson 2000, Kamler et al. 2005). Scent-marking serves to communicate territories among conspecifics, and resident coyotes and wolves strategically mark via urination and defecation at higher rates than do transients, with alpha pairs often exhibiting the highest defecation rates among all cohorts (Rothman and Mech 1979, Gese and Ruff 1997, Barja and List 2014). In contrast, rubbing behavior by canids has been attributed to mate attraction and early courtship, suggesting that rubbing in odorous materials would be advantageous to transients who are actively seeking mates (Ryon et al. 1986, Martin and Farge 1988, Heffernan et al. 2007). Therefore, we speculate that scat sampling may be more likely to detect territorial alpha pairs and other residents, whereas hair sampling may be more likely to detect transients, which would cause the inconsistent individual heterogeneity between detection methods that we found. Given transient individuals have larger home ranges and may be more likely to leave hair samples because of their non-territoriality, this could explain why σ would be estimated larger for the hair observation process. If true, we should expect that previous spatial capture–recapture studies that relied solely on scat transect sampling of coyotes, wolves, and other social and territorial canids may have underestimated total

population density and abundance due to potentially strong individual heterogeneity in λ_0.

The correct model to describe all of these effects would be one with a finite mixture (Pledger 2000) explaining transient versus resident status, with the transients having a larger σ, lower λ_0^s, and higher λ_0^h, and the residents having a smaller σ, higher λ_0^s, and lower λ_0^h. An alternative model to describe differing space use between residents and transients is the model developed by Royle et al. (2016) that allows individual activity centers to move between sampling occasions; however, the data requirements to distinguish between these two models for differential space use are likely much larger than typically available, especially if resident versus transient status is unknown and must be estimated. Given that the model with individual heterogeneity in σ can approximate the model with a subset of activity centers being transient, except for the dependence structure between observations (Royle et al. 2016), we chose to frame the discussion of differential space use in this manner.

A primary limitation of our study was the loss of both scat and hair detections as a consequence of samples containing insufficient DNA. Theoretically, evidence for differential individual heterogeneity in λ_0 could possibly have been induced by individual heterogeneity in DNA amplification rates rather than the aforementioned ecological and behavioral characteristics, although we are unaware of any mechanisms that could directly cause this. The loss of potential detections because of DNA degradation is likely similar to randomized subsampling, to which spatial capture–recapture models appear to be much more robust compared to traditional non-spatial capture–recapture models (Augustine et al. 2014, Murphy et al. 2016). Nevertheless, successful DNA amplification and individual identification rates from fecal samples are often low because the composition of scat includes waste that can inhibit PCR (Long et al. 2008, Lonsinger et al. 2015). The proportion of our fecal samples that could not be species-typed or genotyped (83.9%) were comparable to that reported by Morin et al. (2016), but were higher than reported by Gulsby et al. (2016), Lonsinger et al. (2015), and Mumma et al. (2015) despite our collection and storage methods being identical to those studies. Although based on a small sample size, Ausband et al. (2011) also reported higher DNA amplification and individual identification success rates for hair samples collected via rub pads than we observed (7.8%), and we used identical sampling and storage methods. We also analyzed our scat and hair samples at the same laboratory dedicated to low-quality, low-quantity DNA samples that was used by Ausband et al. (2011), Lonsinger et al. (2015), Mumma et al. (2015), and Morin et al. (2016).

Amplification and PCR success rates are typically highest for scat and hair samples that are collected in very cold and dry climates because warmth and moisture can rapidly degrade DNA (Murphy et al. 2007, Brinkman et al. 2010, Lonsinger et al. 2015). Although we conducted sampling during the coldest winter months, average temperature during sampling at the southerly latitude of our study area was still warm compared to other regions of North America (11°C, range: 5–16°C; NOAA 2017). Our study area also had a subtropical climate that was characterized as being among the most humid areas of North America (average annual relative humidity = 75.9%) and incurred regular precipitation ($\bar{x}$ = 7.49 cm/week during sampling, SE = 2.29; NOAA 2017). Because our sample storage and laboratory methods were identical to other studies that achieved higher DNA amplification success, we posit that the warm, humid climate and wet conditions of our study area caused rapid DNA degradation in samples (Gulsby et al. 2016). Although we checked each rub pad every seven days, more frequent checks may be necessary in areas of similar climatic conditions. Sampling scat transects at more frequent intervals would be unlikely to provide the same benefit, however, because scat accumulation rates along travel routes are slow for coyotes, wolves, and other carnivores that are highly mobile and occupy landscapes at low densities (Lonsinger et al. 2015).

Our results and those of previous studies collectively demonstrate that sparse detection data from noninvasive genetic sampling of social and territorial canids is a prevalent issue that results in generally poor parameter estimate precision (Stansbury et al. 2014, Bozarth et al. 2015, Morin et al. 2016). Assuming the detection patterns that we observed were produced by method-specific

σ parameters (i.e., model SH2), we obtained estimates of coyote density and abundance that were more precise than reported by other studies that also used spatial capture–recapture models (Bozarth et al. 2015, Morin et al. 2016), but were nonetheless poorer than desirable. Uncertainty in λ_0 and σ could be substantially reduced and precision improved by integrating telemetry data from radio-collars, which has been shown to improve the effectiveness of sparse noninvasive detection data (Tenan et al. 2017). Both Mexican gray wolves and red wolves are annually radio-monitored and attempts to estimate their population densities and abundances have either failed because of sparse detection data or resulted in imprecise and possibly biased estimates (Adams et al. 2003, Piaggio et al. 2016, Seamster et al. 2016, Hinton et al. 2017). Employing noninvasive genetic sampling while simultaneously collecting telemetry data could have considerable promise for improving demographic estimates of those and other carnivores that exhibit high degrees of sociality and territoriality. Spatial partial identity models that probabilistically link spatial detections of partial individuality to improve precision of spatial capture–recapture density estimates (Augustine et al. 2018*a*) have been recently extended to incorporate partial genotypes from noninvasive genetic detection data (Augustine et al. 2018*b*). We obtained partial genotypes (≥1 <9 amplified loci) for 16 scat and 21 hair samples, data that could be incorporated to improve parameter estimate precision if those genotypes are reliable or if appropriate error processes are accounted for (e.g., genotyping error; Wright et al. 2009). Nonetheless, we caution that if the patterns we observed were indeed caused by inconsistent individual heterogeneity in λ_0, as postulated, then combining multiple types of noninvasive genetic detection data may be problematic for social and territorial carnivores. These data are typically sparse, modeling individual heterogeneity in λ_0 with sparse detection data is difficult, and positive bias can be introduced in density estimates if individual heterogeneity is not appropriately modeled.

Acknowledgments

This study was funded by Cooperative Agreement Award #F15AC01292 from the U.S. Fish and Wildlife Service. Supplemental funds were provided by Louisiana Department of Wildlife and Fisheries and the University of Kentucky Department of Forestry and Natural Resources. We thank Emily Carrollo and Andrea Petrullo for assistance with data collection and Meaghan Clark and Michelle Keyes for assistance with laboratory genetic analysis. We are grateful for the support from Robert Gosnell, Leopoldo Miranda, and Billy Leonard. We also thank staff at Southwest Louisiana National Wildlife Refuge Complex, Louisiana Ecological Services Office, and Louisiana Department of Wildlife and Fisheries for providing logistical support. *Author contributions*: SMM conceived and designed the study, acquired funding, collected data, analyzed capture–recapture data, and led writing; BCA developed MCMC algorithms and analyzed capture–recapture data; JRA and LPW conducted laboratory genetic analysis; and JJC contributed to study design and acquired supplemental funding. All authors participated in discussion of findings, writing and reviewing of the manuscript, and provided final approval for publication. To the best of our knowledge, no conflict of interest, financial, relational, or other, exists.

Literature Cited

Adams, J. R., B. T. Kelly, and L. P. Waits. 2003. Using faecal DNA sampling and GIS to monitor hybridization between red wolves (*Canis rufus*) and coyotes (*Canis latrans*). Molecular Ecology 12:2175–2186.

Adams, J. R., and L. P. Waits. 2007. An efficient method for screening faecal DNA genotypes and detecting new individuals and hybrids in the red wolf (*Canis rufus*) experimental population area. Conservation Genetics 8:123–131.

Allen, J. J., M. Bekoff, and R. L. Crabtree. 1999. An observational study of coyote (*Canis latrans*) scent-marking and territoriality in Yellowstone National Park. Ethology 105:289–302.

Augustine, B. C., J. A. Royle, M. Kelly, C. Satter, R. Alonso, E. Boydston, and K. Crooks. 2018*a*. Spatial capture-recapture with partial identity: an application to camera traps. Annals of Applied Statistics 12:67–95.

Augustine, B. C., J. A. Royle, S. M. Murphy, R. B. Chandler, J. J. Cox, and M. J. Kelly. 2018*b*. Spatial capture-recapture for categorically marked populations with an application to genetic capture-recapture. bioRxiv:265678. https://doi.org/10.1101/265678

Augustine, B. C., C. A. Tredick, and S. J. Bonner. 2014. Accounting for behavioral response to capture when estimating population size from hair snare

studies with missing data. Methods in Ecology and Evolution 5:1154–1161.

Ausband, D. E., J. Young, B. Fannin, M. S. Mitchell, J. L. Stenglein, L. P. Waits, and J. A. Shivik. 2011. Hair of the dog: obtaining samples from coyotes and wolves noninvasively. Wildlife Society Bulletin 35:105–111.

Barja, I., and R. List. 2014. The role of spatial distribution of faeces in coyote scent marking behavior. Polish Journal of Ecology 62:373–384.

Barrette, C., and F. Messier. 1980. Scent-marking in free-ranging coyotes, *Canis latrans*. Animal Behaviour 28:814–819.

Berger, K. M., E. M. Gese, and J. Berger. 2008. Indirect effects and traditional trophic cascades: a test involving wolves, coyotes, and pronghorn. Ecology 89:818–828.

Bohling, J. H., and L. P. Waits. 2011. Assessing the prevalence of hybridization between sympatric *Canis* species surrounding the red wolf (*Canis rufus*) recovery area in North Carolina. Molecular Ecology 20:2142–2156.

Boitani, L., C. S. Asa, and A. Moehrenschlager. 2004. Tools for canid conservation. Pages 143–162 *in* D. W. McDonald and C. Sillero-Zubiri, editors. Biology and management of wild canids. Oxford University Press, New York, New York, USA.

Bozarth, C. A., B. Gardner, L. L. Rockwood, and J. E. Maldonado. 2015. Using fecal DNA and spatial capture-recapture to characterize a recent coyote colonization. Northeastern Naturalist 22:144–162.

Brinkman, T. J., M. K. Schwartz, D. K. Person, K. L. Pilgrim, and K. J. Hundertmark. 2010. Effects of time and rainfall on PCR success using DNA extracted from deer fecal pellets. Conservation Genetics 11:1547–1552.

Clare, J., S. T. McKinney, J. E. DePue, and C. S. Loftin. 2017. Pairing field methods to improve inference in wildlife surveys while accommodating detection covariance. Ecological Applications 27:2031–2047.

De Barba, M., J. R. Adams, C. S. Goldberg, C. R. Stansbury, D. Arias, R. Cisneros, and L. P. Waits. 2014. Molecular species identification for multiple carnivores. Conservation Genetics Resources 6: 821–824.

Efford, M. G., D. K. Dawson, and C. S. Robbins. 2004. DENSITY: software for analyzing capture-recapture data from passive detector arrays. Animal Biodiversity and Conservation 27:217–228.

Efford, M. G., and G. Mowat. 2014. Compensatory heterogeneity in spatially explicit capture-recapture data. Ecology 95:1341–1348.

Foster, R. J., and B. J. Harmsen. 2012. A critique of density estimation from camera-trap data. Journal of Wildlife Management 76:224–236.

Gese, E. M., and R. L. Ruff. 1997. Scent-marking by coyotes, *Canis latrans*: the influence of social and ecological factors. Animal Behaviour 54:1155–1166.

Gopalaswamy, A. M., J. A. Royle, M. Delampady, J. D. Nichols, K. U. Karanth, and D. W. Macdonald. 2012. Density estimation in tiger populations: combining information for strong inference. Ecology 93:1741–1751.

Gulsby, W. D., C. H. Killmaster, J. W. Bowers, J. S. Laufenberg, B. N. Sacks, M. J. Statham, and K. V. Miller. 2016. Efficacy and precision of fecal genotyping to estimate coyote abundance. Wildlife Society Bulletin 40:792–799.

Heffernan, D. J., W. F. Andelt, and J. A. Shivik. 2007. Coyote investigative behavior following removal of novel stimuli. Journal of Wildlife Management 71:587–593.

Hinton, J. W., G. C. White, D. R. Rabon Jr, and M. J. Chamberlain. 2017. Survival and population size estimates of the red wolf. Journal of Wildlife Management 81:417–428.

Hjort, N. L., F. A. Dahl, and G. H. Steinbakk. 2006. Post-processing posterior predictive *p* values. Journal of the American Statistical Association 101:1157–1174.

Holmes, N. G., H. F. Dickens, H. L. Parker, M. M. Binns, C. S. Mellersh, and J. Sampson. 1995. Eighteen canine microsatellites. Animal Genetics 26: 131–132.

Homer, C., J. Dewitz, L. Yang, S. Jin, P. Danielson, G. Xian, J. Coulston, N. Herold, J. Wickham, and K. Megown. 2015. Completion of the 2011 National Land Cover Database for the conterminous United States – representing a decade of land cover change information. Photogrammetric Engineering and Remote Sensing 81:345–354.

Kamler, J. F., W. B. Ballard, P. R. Lemons, R. L. Gilliland, and K. Mote. 2005. Home range and habitat use of coyotes in an area of native prairie, farmland and CRP fields. American Midland Naturalist 153: 396–404.

Kamler, J. F., and P. S. Gipson. 2000. Space and habitat use by resident and transient coyotes. Canadian Journal of Zoology 78:2106–2111.

Kays, R., A. Curtis, and J. J. Kirchman. 2009. Rapid adaptive evolution of northeastern coyotes via hybridization with wolves. Biology Letters. https://doi.org/10.1098/rsbl.2009.0575

Letnic, M., and W. J. Ripple. 2017. Large-scale responses of herbivore prey to canid predators and primary productivity. Global Ecology and Biogeography 26:860–866.

Levi, T., and C. C. Wilmers. 2012. Wolves-coyotes-foxes: a cascade among carnivores. Ecology 93: 921–929.

Linden, D. W., A. P. K. Siren, and P. J. Jenkins. 2017. Integrating telemetry data into spatial capture-recapture modifies inferences on multi-scale resource selection. bioRxiv:131144. https://doi.org/10.1101/131144

Long, R. A., P. MacKay, J. Ray, and W. Zielinski. 2008. Noninvasive survey methods for carnivores. Island Press, Washington, D.C., USA.

Lonsinger, R. C., E. M. Gese, S. J. Dempsey, B. M. Kluever, T. R. Johnson, and L. P. Waits. 2015. Balancing sample accumulation and DNA degradation rates to optimize noninvasive genetic sampling of sympatric carnivores. Molecular Ecology Resources 15:831–842.

Lonsinger, R. C., E. M. Gese, R. N. Knight, T. R. Johnson, and L. P. Waits. 2016. Quantifying and correcting for scat removal in noninvasive carnivore scat surveys. Wildlife Biology 22:45–54.

López-Bao, J. V., R. Godinho, C. Pacheco, F. J. Lema, E. García, L. Llaneza, V. Palacios, and J. Jiménez. 2018. Toward reliable population estimates of wolves by combining spatial capture-recapture models and non-invasive DNA monitoring. Scientific Reports 8:2177.

Mac, M. J., P. A. Opler, C. E. Puckett Haecker, and P. D. Doran. 1998. Status and trends of the nation's biological resources. Volumes 1 and 2. U.S. Geological Survey, Reston, Virginia, USA.

Martin, D. J., and D. B. Farge. 1988. Field evaluation of a synthetic coyote attractant. Wildlife Society Bulletin 16:390–396.

Mellersh, C. S., A. A. Langston, G. M. Acland, M. A. Fleming, K. Ray, N. A. Wiegand, L. V. Francisco, M. Gibbs, G. D. Aguirre, and E. A. Ostrander. 1997. A linkage map of the canine genome. Genomics 46:326–336.

Moehlman, P. D. 1989. Intraspecific variation in canid social systems. Pages 143–163 *in* J. L. Gittleman, editor. Carnivore behavior, ecology, and evolution. Springer-Science, Boston, Massachusetts, USA.

Morin, D. J., M. J. Kelly, and L. P. Waits. 2016. Monitoring coyote population dynamics with fecal DNA and spatial capture-recapture. Journal of Wildlife Management 80:824–836.

Mumma, M. A., C. Zieminski, T. K. Fuller, S. P. Mahoney, and L. P. Waits. 2015. Evaluating noninvasive genetic sampling techniques to estimate large carnivore abundance. Molecular Ecology Resources 15:1133–1144.

Murphy, S. M., B. C. Augustine, W. A. Ulrey, J. M. Guthrie, B. K. Scheick, J. W. McCown, and J. J. Cox. 2017. Consequences of severe habitat fragmentation on density, genetics, and spatial capture-recapture analysis of a small bear population. PLoS ONE 12:e0181849.

Murphy, S. M., J. J. Cox, B. C. Augustine, J. T. Hast, J. M. Guthrie, J. Wright, J. McDermott, S. C. Maehr, and J. H. Plaxico. 2016. Characterizing recolonization by a reintroduced bear population using genetic spatial capture-recapture. Journal of Wildlife Management 80:1390–1407.

Murphy, M. A., K. C. Kendall, A. Robinson, and L. P. Waits. 2007. The impact of time and field conditions on brown bear (*Ursus arctos*) faecal DNA amplification. Conservation Genetics 8:1219–1224.

NOAA. 2017. Climate data online: Lake Charles, Louisiana. National Oceanic and Atmospheric Administration, Silver Spring, Maryland, USA. https://www.ncdc.noaa.gov/cdo-web/

Ostrander, E. A., G. F. Sprague, and J. Rine. 1993. Identification and characterization of dinucleotide repeat $(CA)_n$ markers for genetic mapping in dog. Genomics 16:207–213.

Peakall, R., and P. E. Smouse. 2012. GenAlEx 6.5: genetic analysis in Excel. Population genetic software for teaching and research – an update. Bioinformatics 28:2537–2539.

Piaggio, A. J., C. A. Cariappa, D. J. Straughan, M. A. Neubaum, M. Dwire, P. R. Krausman, W. B. Ballard, D. L. Bergman, and S. W. Breck. 2016. A noninvasive method to detect Mexican wolves and estimate abundance. Wildlife Society Bulletin 40: 321–330.

Pledger, S. 2000. Unified maximum likelihood estimates for closed capture-recapture models using mixtures. Biometrics 56:434–442.

Popescu, V. D., P. Valpine, and R. A. Sweitzer. 2014. Testing the consistency of wildlife data types before combining them: the case of camera traps and telemetry. Ecology and Evolution 4:933–943.

R Core Team. 2018. R: a language and environment for statistical computing. R Foundation for Statistical Computing, Vienna, Austria.

Robins, J. M., A. van der Vaart, and V. Ventura. 2000. Asymptotic distribution of p values in composite null models. Journal of the American Statistical Association 95:1143–1156.

Rothman, R. J., and L. D. Mech. 1979. Scent-marking in lone wolves and newly formed pairs. Animal Behaviour 27:750–752.

Royle, J. A., R. B. Chandler, R. Sollmann, and B. Gardner. 2014. Spatial capture-recapture. Academic Press-Elsevier, Oxford, UK.

Royle, J. A., R. B. Chandler, C. C. Sun, and A. K. Fuller. 2013. Integrating resource selection information with spatial capture-recapture. Methods in Ecology and Evolution 4:520–530.

Royle, J. A., A. K. Fuller, and C. Sutherland. 2016. Spatial capture-recapture models allowing Markovian transience or dispersal. Population Ecology 58:53–62.

Royle, J. A., K. U. Karanth, A. M. Gopalaswamy, and N. S. Kumar. 2009. Bayesian inference in camera trapping studies for a class of spatial capture-recapture models. Ecology 90:3233–3244.

Ryon, J., J. C. Fentress, F. H. Harrington, and S. Bragdon. 1986. Scent rubbing in wolves (*Canis lupus*): the effect of novelty. Canadian Journal of Zoology 64:573–577.

Seamster, M., C. Inscore, and D. T. Cobb. 2016. Occupancy of large canids in eastern North Carolina – a pilot study. Journal of the Southeastern Association of Fish and Wildlife Agencies 3:280–285.

Seddon, J. 2005. Canid-specific primers for molecular sexing using tissue or non-invasive samples. Conservation Genetics 6:147–149.

Sollmann, R., B. Gardner, R. B. Chandler, D. B. Shindle, D. P. Onorato, J. A. Royle, and A. F. O'Connell. 2013*a*. Using multiple data sources provides density estimates for endangered Florida panther. Journal of Applied Ecology 50:961–968.

Sollmann, R., B. Gardner, A. W. Parsons, J. J. Stocking, B. T. McClintock, T. R. Simons, K. H. Pollock, and A. F. O'Connell. 2013*b*. A spatial mark-resight model augmented with telemetry data. Ecology 94:553–559.

Sollmann, R., N. M. Torres, M. M. Furtado, A. T. Almeida Jacomo, F. Palomares, S. Roques, and L. Silveira. 2013*c*. Combining camera-trapping and noninvasive genetic data in a spatial capture-recapture framework improves density estimates for the jaguar. Biological Conservation 167:242–247.

Stansbury, C. R., D. E. Ausband, P. Zager, C. M. Mack, C. R. Miller, M. W. Pennell, and L. P. Waits. 2014. A long-term population monitoring approach for a wide-ranging carnivore: noninvasive genetic sampling of gray wolf rendezvous sites in Idaho, USA. Journal of Wildlife Management 78:1040–1049.

Stenglein, J. L., M. De Barba, D. E. Ausband, and L. P. Waits. 2010. Impacts of sampling location within a faeces on DNA quality in two carnivore species. Molecular Ecology Resources 10:109–114.

Tenan, S., P. Pedrini, N. Bragalanti, C. Groff, and C. Sutherland. 2017. Data integration for inference about spatial processes: a model-based approach to test and account for data inconsistency. PLoS ONE 12:e0185588.

Venables, W. N., and B. D. Ripley. 2002. Modern applied statistics with S. Fourth edition. Springer, New York, New York, USA.

Waits, L. P., and D. Paetkau. 2005. Noninvasive genetic sampling tools for wildlife biologists: a review of applications and recommendations for accurate data collection. Journal of Wildlife Management 69:1419–1433.

Wells, M. C., and M. Bekoff. 1981. An observational study of scent-marking in coyotes, *Canis latrans*. Animal Behaviour 29:332–350.

Wright, J. A., R. J. Barker, M. R. Schofield, A. C. Frantz, A. E. Byrom, and D. M. Gleeson. 2009. Incorporating genotype uncertainty into mark-recapture-type models for estimating abundance using DNA samples. Biometrics 65:833–840.

Supporting Information

Additional Supporting Information may be found online at: http://onlinelibrary.wiley.com/doi/10.1002/ecs2.2479/full